(3)

AIAA Paper
No. 74-627

TRANSITION REYNOLDS NUMBER COMPARISONS
IN SEVERAL MAJOR TRANSONIC TUNNELS

by
N. S. DOUGHERTY, JR.
ARO, Incorporated
Arnold Air Force Station, Tennessee
and
FRANK W. STEINLE, JR.
NASA/Ames Research Center
Moffett Field, California

29 JUL 1974
ENGINEERING LIBRARY
ST. LOUIS

AIAA PAPER 74-627

AAIA 8th Aerodynamic Testing Conference

BETHESDA, MARYLAND / JULY 8-10, 1974

First publication rights reserved by American Institute of Aeronautics and Astronautics. 1290 Avenue of the Americas, New York, N. Y. 10019. Abstracts may be published without permission if credit is given to author and to AIAA. (Price: AIAA Member $1.50. Nonmember $2.00).

Note: This paper available at AIAA New York office for six months; thereafter photoprint copies are available at photocopy prices from AIAA Library, 750 3rd Avenue, New York, New York 10017

M74-14126

TRANSITION REYNOLDS NUMBER COMPARISONS IN SEVERAL MAJOR TRANSONIC TUNNELS*

N. S. Dougherty, Jr.**
ARO, Inc., Arnold Air Force Station, Tennessee

and

Frank W. Steinle, Jr.†
NASA/Ames Research Center, Moffett Field, California

Abstract

Boundary-layer transition and test section environmental noise data were acquired in six major transonic wind tunnels as a part of a broader correlation of the effect of free-stream disturbances on transition Reynolds number. The data were taken at comparative test conditions on a sharp, smooth 10-deg included-angle cone. It was found that aerodynamic noise sources within the test section were the dominant sources of unsteadiness and that transition Reynolds number provided a good indicator for the resulting degradation in flow quality. Amplitudes, frequency composition, directivity, and origin of these disturbances are described.

I. Introduction

In the past several years there has grown an increasing awareness that the dynamic flow environment in a wind tunnel is influencing aerodynamic test results. With today's increasing needs for improved accuracy in results and expanding scope of test requirements has come the need for better definition of the wind tunnel dynamic flow environment in order that the quality of testing might be improved.

The best indicators of flow quality in a given wind tunnel are:

1. the variations in Mach number,
2. the variations in flow angularity, and
3. model transition Reynolds number.

It is well known that transition Reynolds number is affected by free-stream noise and turbulence levels, model vibrations, heat transfer between the model and the free stream, and the condensation of moisture from the free stream. It is also well known that transition Reynolds number is influenced greatly by the local velocity and pressure gradients about a model and local model-generated disturbances. Morkovin[1,2] has provided an overview of the extensive data available from research on transition and points out the wide disparity in results. Still, there is no fully adequate universal correlation of transition Reynolds numbers as measured in wind tunnels or between wind tunnels and free flight. Indeed, there is still a lack of understanding of the detailed nature of transition, although much progress has been made through the use of linear stability theory as described in Ref. 3, for example. There is an advantage to acquiring transition data on bodies of only simple geometry, i.e., slender cone and planar. But as pointed out by Morkovin, it is essential that an adequate documentation of the flow environment be made when performing experiments on natural transition because of the strong influence of the environment on the results.

Transition Reynolds number, therefore, can be used as an indicator for the dynamic aspects of the flow quality in a wind tunnel. This is in much the same manner that the drag data on the "turbulence sphere" were used in low-speed wind tunnels (less than 0.3 Mach number) to obtain the "turbulence factor." The "turbulence factor" was defined as the effective increase in Reynolds number determined from differences in critical drag Reynolds number from the known reference value in free air. Pope gives a value of 1.4 in Ref. 4 for this "turbulence factor" determined from spheres where the air possibly has too much turbulence for good test results. When measurements of transition Reynolds number were first made on models in supersonic wind tunnels (Ref. 5, for example) there appeared to be trends with tunnel size, Mach number, and unit Reynolds number. Pate and Schueler showed that most of the observed variations on planar and cone models[6,7] could be explained by the variations in aerodynamic noise level radiated from the tunnel wall boundary layer, which varies as the boundary-layer properties vary with Mach number and unit Reynolds number. They developed an empirical correlation from data acquired in some ten different tunnels at Mach numbers from 3.0 to 8.0. This correlation used only the skin friction and the displacement thickness of the wall boundary layer to characterize the noise strength. The tunnel

*The research reported herein was conducted by the Arnold Engineering Development Center, Air Force Systems Command. Research results were obtained by personnel of ARO, Inc., Contract Operator at AEDC. Further reproduction to satisfy the needs of the U. S. Government is authorized.

**Research Engineer, Member AIAA.

†Research Scientist, Member AIAA.

size variation appeared in radiation laws for wall area, distance from the wall, etc. Accordingly, lowest transition Reynolds numbers occurred in the smallest supersonic tunnels.

The present study is concerned with the dynamic flow quality in transonic tunnels. Numerous studies in transonic tunnels have revealed the presence of additional disturbances in transonic test section flow, over and above wall boundary-layer radiation, most of which are of acoustic origin and are associated with the ventilated test section walls required to establish Mach numbers near 1.0 and to reduce supersonic wave disturbances. Examples of the various types of acoustic disturbances found in several transonic tunnels are given in Refs. 8 through 12. In view of the present-day requirements for transonic testing, there is a particularly urgent need for critical evaluation of the dynamic environment in transonic tunnels. It was shown by Mabey[13] that flow unsteadiness at subsonic and transonic speeds can affect both steady-state and dynamic test results. Mabey gives a proposed dynamic criterion for the maximum acceptable level of unsteadiness in the flow for transonic buffet evaluation which is exceeded at some test conditions in many existing transonic tunnels.

Transition data are being acquired on a slender cone fabricated by ARO, Inc., at the USAF Arnold Engineering Development Center (AEDC). At each test condition, simultaneous measurements of the free-stream fluctuating pressure level are made using two flush-mounted microphones on the surface of the cone. Data were first acquired in the two 16-ft Propulsion Wind Tunnels (transonic and supersonic) and in the 4-ft Aerodynamic Wind Tunnel at AEDC. With the cooperation of the National Aeronautics and Space Administration (NASA) and the U.S. Air Force, additional testing has been performed in several tunnels at the Ames and Langley Research Centers. A list of participating tunnels to date including the Calspan Corp. and Naval Ship Research and Development Center tunnels is given in Table 1. These tests have included a variety of subsonic, transonic, and supersonic variable density and atmospheric tunnels of varied size and geometry to obtain as general a correlation as possible of the effect of aerodynamic noise on transition. Seven of these tunnels are in the United Kingdom, France, and the Netherlands for correlation among tunnels used in common Western European aircraft systems development. With the exception of the industrial manufacturer tunnels, the list in the U. S. now includes most of the major domestic tunnels where the cone tests have provided a common basis of comparison using a standard model with standardized test procedures.

Treon, Steinle, et al.[14] showed that best agreement of static aerodynamic data derived from tests of a high-subsonic speed transport aircraft model at cruise Mach

Table 1 List of tunnels participating in correlation study

*AEDC 16-ft Transonic Propulsion Wind Tunnel
AEDC 16-ft Supersonic Propulsion Wind Tunnel
*AEDC 4-ft Transonic Aerodynamic Wind Tunnel
*NASA/Ames 11-ft Transonic Wind Tunnel
*NASA/Ames 14-ft Transonic Wind Tunnel
Nasa/Ames 12-ft Pressure Tunnel
*NASA/Langley 8-ft Transonic Pressure Tunnel
*NASA/Langley 16-ft Transonic Tunnel
NASA/Langley 16-ft Transonic Dynamics Tunnel
Calspan 8-ft Transonic Tunnel
Naval Ship R & D Center 7- x 10-ft Transonic Tunnel
RAE 8- x 8-ft Supersonic Wind Tunnel
RAE 8- x 6-ft Transonic Wind Tunnel
RAE 3- x 4-ft Supersonic Wind Tunnel
ARA, LTD. 9- x 8-ft Transonic Tunnel
ONERA 6- x 6-ft S-2MA Transonic Tunnel
**ONERA 2.56- x 1.83-ft S-3MA Transonic Tunnel
**NLR 6.55 x 5.28-ft High Speed Tunnel

*Present Study
**Background Noise Data Only

numbers in the AEDC 16-ft Transonic Propulsion Wind Tunnel, the NASA/Ames Research Center 11-ft Transonic Wind Tunnel, and the Calspan 8-ft Transonic Tunnel was obtained by accounting for relative Reynolds number effects between facilities. Here, the relative Reynolds number effects were defined using the AEDC 10-deg transition cone results in each of these tunnels. For example, it is shown in Ref. 14 that a significant improvement of the correlation achieved between these tunnels was obtained by adjusting the drag coefficient at zero-normal-force angle of attack with a correction factor derived from the cone transition Reynolds number data. These results of Ref. 14 substantiate the need for developing a method for predicting these corrections to Reynolds number to improve the extrapolation of wind tunnel test results to full-scale flight conditions, i.e., a "turbulence factor" for transonic tunnels. Although the "effect" associated with these differences in transition characteristics between tunnels is of prime importance in adjusting the data, the "cause" is of particular significance since it relates directly to predicting the "effect" in new and different facilities. This illustration of improvement in agreement of results between transonic facilities suggests the use of transition Reynolds number for such corrections to be both technically appropriate and productive.

The purpose of this paper is to present the cone test results in the six transonic tunnels of the USAF and NASA indicated in Table 1. These were comparative tests at matched flow conditions which illustrate the variance in transition Reynolds numbers that occurs in these particular transonic tunnels currently employed in new aircraft systems development. Analysis of data acquired in other tunnels continues and will be reported

in the future in a broader correlation of results.

II. Apparatus

Calibration Model

The transition calibration model is shown in Fig. 1 and consists of a smooth, sharp, 10-deg included-angle cone which was machined from two solid pieces of stainless steel, heat treated, assembled, finish ground, and polished to a surface finish of 8 to 12 microinch root-mean-square (μ in.-rms) waviness. The tip bluntness is equivalent to less than a 0.005-in. diameter. Length of the cone is 3 ft.

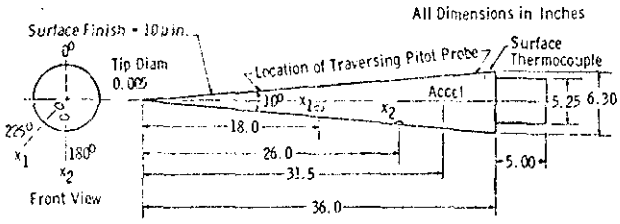

Fig. 1 Calibration model.

The cone is equipped with a traversing pitot probe for transition detection, two surface-mounted 1/4-in.-diam condenser microphones,‡ a surface temperature thermocouple peened just beneath the surface near the base of the cone, and a vertical-axis-sensing piezoelectric accelerometer for assessing microphone acceleration sensitivity, which in all tunnels to date has been found to be insignificant.

The traversing probe is equipped with a 1/8-in.-diam strain-gage-type pressure transducer close-coupled to the sensing tube. The probe tip rides along the surface of the cone and has a tip opening height of nominally 0.005 in., allowing the survey of very thin boundary layers on the forward portion of the cone.

The cone has been physically aligned to the geometric centerline of each wind tunnel. A sufficient number of tests for transition sensitivity to small angles of attack and sideslip have been performed to assess the effects of crossflow on the measured transition location. All of the data presented in this paper are at an assumed zero-degree incidence with the test section flow. Use of the cone surface thermocouple is for verification of thermal equilibrium between the model and the free stream. The thermocouple was installed for tests in only ten of the wind tunnels to date. It is assumed in all of the results presented in this paper that the data were acquired at adiabatic wall conditions for the cone. Efforts were made to hold tunnel total temperature near constant where possible and to allow sufficient time for heat transfer to be minimized in the conduct of testing.

Facilities

General features of the six subject tunnels are given in Table 2. In addition to the range of test section size from 4-ft square to 16-ft square and, in the case of the NASA/LRC 16-ft transonic tunnel, 15.5-ft octagonal, these particular tunnels provide an interesting comparison for three basic test section ventilation concepts. The two AEDC tunnels have the pure perforated-wall ventilation configuration using 60-deg inclined differential resistant holes developed for optimized cancellation of model-generated shock and expansion waves at Mach numbers near 1.2. The AEDC 16-ft transonic Propulsion Wind Tunnel has 3/4-in.-diam holes in a pattern that gives a uniform 6-percent porosity. The AEDC 4-ft Aerodynamic Wind Tunnel has 1/2-in.-diam holes with a sliding backing plate for varying the porosity. A nominal 5- or 6-percent porosity is used at subsonic Mach numbers and above Mach 1.2. In the range of Mach numbers from 1.0 to 1.2, a reduced porosity schedule (varied with Mach number) gives improved wave cancellation. The two LRC tunnels use coarsely spaced longitudinal slots at nominally 4- to 5-percent porosity designed for minimized subsonic wall interference and contoured for optimized supersonic axial Mach number distribution. This purely slotted-wall configuration, therefore, provides direct contrast with the purely perforated-wall configuration. The two ARC tunnels use finely spaced longitudinal slots at 5.6-percent porosity with corrugated metal inserts that, in effect, combine the features of the purely slotted and purely perforated-wall configurations.

Table 2 General features of the tunnels

Tunnel	Test Section Size, ft	Shape	Configuration	Density
AEDC 4T	4.0	Square	Perforated	Variable
AEDC 16T	16.0	Square	Perforated	Variable
NASA/ARC 11TWT	11.0	Square	Slotted	Variable
NASA/ARC 14TWT	13.8 x 13.5	Square	Slotted	Atmospheric
NASA/LRC 8TPT	7.1	Square	Slotted	Variable
NASA/LRC 16TT	15.6	Octagonal	Slotted	Atmospheric

III. Experimental Measurements

Transition Location

Transition location as measured by the traversing probe will be defined as shown in the typical pitot pressure profiles in Fig. 2. The laminar boundary layer exhibits a decreasing steady pitot pressure to some minimum value. (This is with fluctuating components removed by a 2-Hz low-pass filter,

‡Quarter-inch microphones were used in all of these tests except for those in the two NASA/Langley Research Center tunnels where 1/8-in. strain-gage pressure transducers were used.

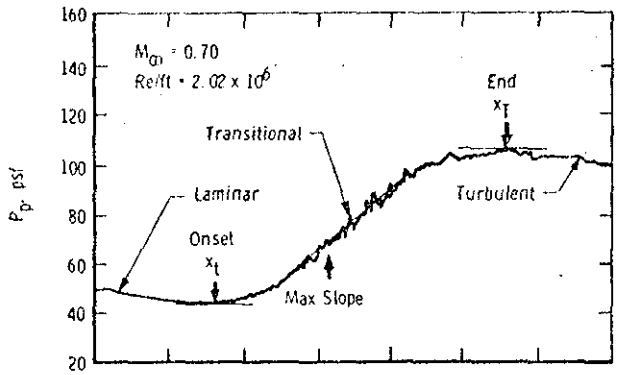

a. Low-pass filtered

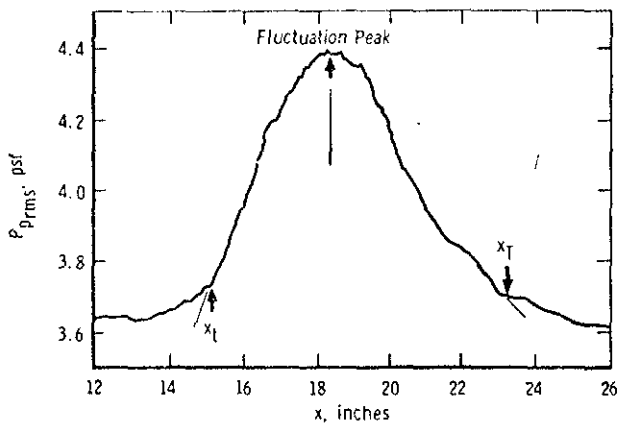

b. High-pass filtered

Fig. 2 Typical boundary layer pitot profile.

Fig. 2a). Taking the tangent point at the minimum value of pitot pressure gives the x-location to be defined as the onset of transition location, x_t. In the transition region there is a sudden increase in steady pitot pressure to a maximum value with increasing x-distance, followed by a decay in pressure. Taking the tangent point at the maximum value of pitot pressure gives the x-location to be defined as the end of transition location, x_T. For x-distance greater than this end of transition point, the boundary layer is considered to have attained fully developed turbulent flow. The fluctuating portion of the traversing probe transducer signal, high-pass filtered above 2 Hz, is shown in Fig. 2b. The frequency response of the probe-transducer system is relatively low, 3 db point at 30 Hz; however, there is sufficient low-frequency composition of the turbulent bursts during transition to indicate a rise in the integrated true-root-mean-square level of pressure fluctuations as seen in Fig. 2b. The rms level attains a well-defined peak near the midregion of transition at a location corresponding to the maximum slope of the steady pressure profile. This peak in rms signal has been used by some investigators to define transition. There is some question about precisely where transition begins. The filtered fluctuating portion of the probe transducer signal has consistently shown a discernible growth in oscillations slightly ahead of the minimum point in the steady-pressure profile. The growth of oscillations is first exponential as indicated in Fig. 2b followed by linear growth with increasing x-distance to the peak in rms amplitude midway through transition. In this paper, however, the above-defined onset and end of transition points based on the steady pitot pressure will be used for the calculation of transition Reynolds numbers.

Onset of transition Reynolds number, Re_t, is defined as follows

$$Re_t = Re/ft \cdot x_t \qquad (1)$$

and the end of transition Reynolds number, Re_T, as

$$Re_T = Re/ft \cdot x_T \qquad (2)$$

These length Reynolds numbers use the free-stream unit Reynolds number per foot, $Re/ft = U_\infty/\nu_\infty$; however, it is recognized that local surface flow conditions are altered at supersonic speeds by the presence of the bow shock, which becomes attached at approximately $M_\infty = 1.02$. The pitot profiles were recorded in analog form on "X-Y" plotters using a forward moving traverse at all times, because there is appreciable hysteresis when traversing rearward as compared to traversing forward. Greatest uncertainty in measurements lies in the subjective interpretation of the pitot profiles which can be read with statistical confidence to approximately 0.5 in., 3σ. The end of transition point has been more commonly used by transition investigators, because it is more clearly definable than the onset point. The end of transition point will be used for the basic tunnel comparison. Onset of transition data are given in addition in the correlation of results in the attempt to establish the influence of noise on the point where laminar flow breakdown occurs.

Background Noise

The most direct measurement of the test section background noise level is with a flush-mounted microphone on the surface of the model. This measurement is taken to be the sound pressure level at the tunnel centerline to which the test model is exposed. In many of the wind tunnels in which the cone has been tested, simultaneous measurements have also been taken on the test section wall opposite the model microphones. There have been small differences in these measurements on the wall compared to those on the cone; but, use of the wall microphone once correlated to the cone has allowed a permanent monitoring station for assessment of the effect of any future changes in the tunnel following the cone test.

Ideally, the fluctuating pressure measurement should be taken under a laminar boundary layer, free of local turbulence influence. However, in practice it has been found for most of the transonic tunnels

that there is little difference on the cone between readings under a laminar or turbulent boundary layer. But, there is a large difference (up to a factor of two or more) if the microphone happens to be under the transition zone where the local disturbances associated with the transition process are recorded in addition to the free-stream background disturbances. Separation of the two microphones by an 8-in. axial distance, as shown in Fig. 1, ensures that either one or the other microphone will not be in the transition zone, thus giving a reasonably valid background noise measurement. The 45-deg difference in roll orientation of the two cone microphones (see Fig. 1) has given no appreciable differences in measured amplitudes.

The microphones have been calibrated in-place in each tunnel by physical application of a 1-kHz sinusoidal pressure wave at either a 140- or 160-db sound pressure level (Ref. 0.0002 μbar) with estimated uncertainty of ±0.5 db at 160 db. Background noise levels have been recorded on magnetic tape to 10 kHz or 20 kHz frequency response. Most of the energy (>95 percent) has been found to occur within 10-kHz bandwidth and >98 percent within 20 kHz in most of the tunnels. Background sound pressure levels have been recorded using a true rms voltmeter with 1-sec time constant and approximately 10-sec averaging time over the full recording bandwidth. On the low-frequency end, the 1/4-in. condenser microphones begin to exhibit roll-off at 50 Hz; however, disturbances as low in frequency as 10 Hz have been identifiable.

The time-averaged, frequency-integrated, true-root-mean-square fluctuating pressure represents the square root of the power spectral density over the full recording bandwidth and is thus defined as $\sqrt{\tilde{p}^2}$. The fluctuating pressure has then been normalized by q_∞ to fluctuating pressure coefficient, ΔC_p, defined as follows:

$$\Delta C_p = \frac{\sqrt{\tilde{p}^2}}{q_\infty} \times 100, \text{ percent} \qquad (3)$$

It is recognized that there are vorticity fluctuations (turbulence) in the free-stream flow in addition to the sound waves. Pure vorticity fluctuations are not accounted for by the microphone measurements; however, a portion of the free-stream velocity fluctuations are sound-wave coupled. These are accounted for in the measurement of fluctuating pressure if a plane-wave assumption is made for the propagation of the sound and the further assumption that the sound waves are isentropic. Defining turbulence intensity (TI) as the rms fluctuating velocity percentage of free-stream steady velocity over the same bandwidth, a rudimentary estimate is made for the relationship between fluctuating pressure coefficient (ΔC_p) and turbulence intensity (TI) that

$$\Delta C_p = \frac{2}{M_\infty} (\text{TI}) \qquad (4)$$

Vorticity fluctuations are usually traceable to conditions existing within and upstream of the stilling chamber. Direct measurements of turbulence intensity can be made using hot film or hot-wire anemometers both in the test section and in the stilling chamber. Such measurements are difficult to make and to interpret and should include all three Cartesian-coordinate axes of velocity fluctuation as the isotropic assumption is not always valid. Illustration of this observation that the turbulence may not be isotropic is taken from results by Uberoi given in Fig. 3. Uberoi found that there is dissimilar attenuation of stilling chamber turbulence while passing through the nozzle contraction for axial and cross-stream components. Figure 3 presents the effect of the contraction on the absolute intensity of the filaments and shows the cross-stream components to be amplified with maximum amplification near Mach 1.0. For this reason, stilling chamber vorticity fluctuations at transonic speeds cannot be ignored. Some turbulence data

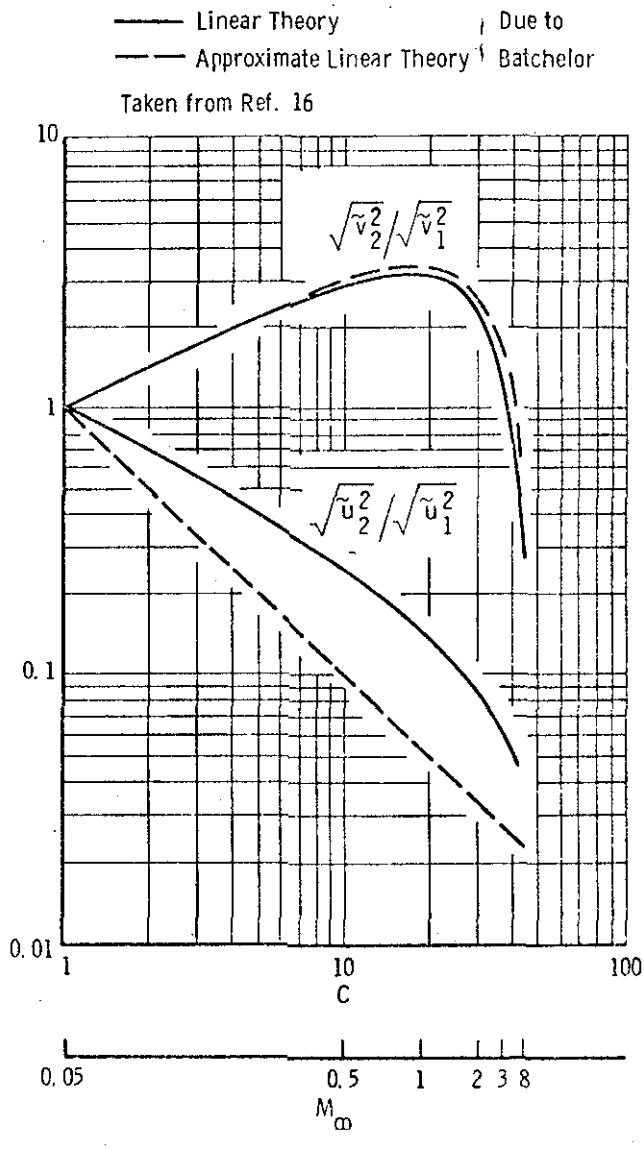

Fig. 3 Effect of nozzle contraction on turbulence transmissibility.

(unpublished) are available for the AEDC 16-ft transonic propulsion wind tunnel and the NASA/Langley 8-ft transonic pressure tunnel and 16-ft transonic tunnel. The data from all three of these tunnels suggest appreciable anisotropy of turbulence in the transonic test sections with maximum amplitudes on the order of 1.0-percent TI at Mach 1.0.

In contrast to this level of turbulence intensity, the cone ΔC_p data have revealed considerably higher amplitudes from acoustic sources than would be expected even from comparatively large stilling chamber turbulence such that it is a safe assumption that the ΔC_p measurements account for most of the free-stream disturbances affecting transition Reynolds number. Thus, in this paper, the fluctuating pressure coefficient (ΔC_p) alone will be used to correlate the transition data.

IV. Results

AEDC 4T

The 10-deg cone results obtained in the AEDC 4-ft Aerodynamic Wind Tunnel (AEDC 4T) are presented in Fig. 4. The dominating disturbances are whistling tones emanating from the perforated walls and maximum in amplitude (ΔC_p) at Mach numbers near 0.8 and near 1.2. The maximum amplitude recorded at maximum q_∞ was 152 db. These tones have been identified as edgetones which are nearly discrete in frequency, standing out as much as 20 db above the background random noise. They are caused by interaction of a vortex forming over each hole with the sharp trailing edge of the hole. Varied suction and porosity (τ) give rise to differing harmonic content of the noise. Documented here are the end of transition Reynolds numbers at corresponding ΔC_p levels at varied Mach number and constant unit Reynolds numbers of 2.0×10^6, 3.0×10^6, and 4.0×10^6. Tunnel total temperature, T_t, was held near constant at 125°F and the total pressure, p_t, varied to obtain this unit Reynolds number variation.

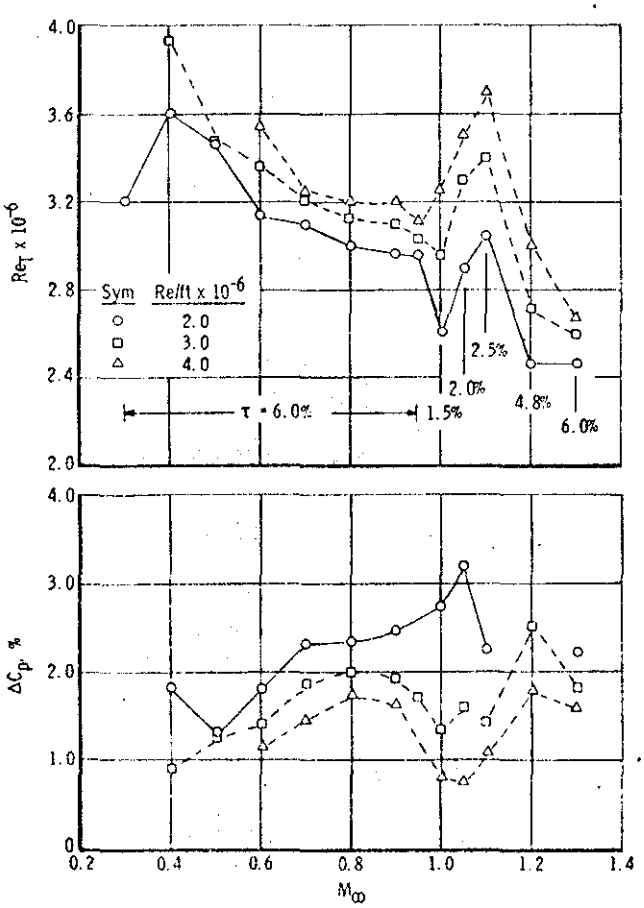

Fig. 4 Noise and Re_T variation in AEDC 4T.

AEDC 16T

The cone results obtained in the AEDC 16-ft Transonic Propulsion Wind Tunnel (AEDC 16T) are presented in Fig. 5. There is a sharply defined resonance condition at 0.709 Mach number produced by the first-stage (fundamental) edgetone from the perforated walls. The degree of amplification in ΔC_p is reduced as unit Reynolds number is increased from 2.0×10^6 to 6.0×10^6 as shown in Fig. 5. This was at near constant 120°F total temperature and varied total pressure as in AEDC 4T. The amplification is produced by the edgetone frequency coinciding with the twelfth fundamental natural reverberation frequency of the test section at nominally 560 Hz. The reverberation frequency is calculated from the following expression:

$$f_n^2 = \frac{m^2 \, c_\infty^2}{4 \, L_x^2} \left(1 - M_\infty^2\right) \qquad (5)$$

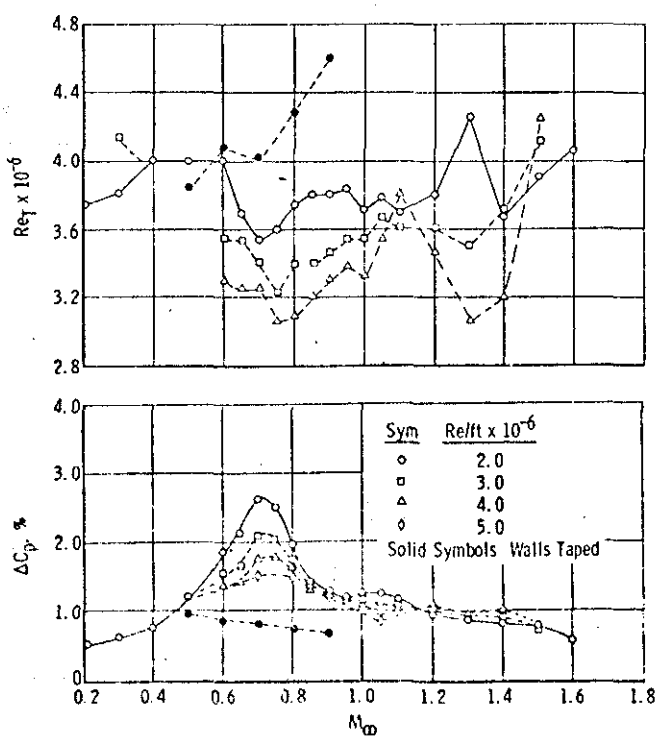

Fig. 5 Noise and Re_T variation in AEDC 16T.

where L_x is the cross-sectional dimension of the test section, 16.0 ft; m is the number of waves involved, 24. This is a pure transverse mode of resonance where oblique initial and reflected waves are in phase and reinforce the vortex oscillation over each hole. Equation (5) is also given in Refs. 8 and 17 to explain discrete tone resonances where the sound waves were reinforced due to reflections at the walls. It is this characteristic type of resonance at some particular high subsonic Mach number that is responsible for the presence of large acoustic disturbances in most transonic tunnels. The resonance condition in AEDC 16T was effectively eliminated by taping the inside surfaces of all four walls closed. Lower noise and higher corresponding transition Reynolds numbers at a unit Reynolds number of 2.0×10^6 are evident with the walls taped for Mach numbers between 0.5 and 0.9.

The edgetone frequencies for the perforated walls generally increase with Mach number and were found to be correlated by the following expression for Strouhal numbers nondimensionalized by the free-stream velocity:

$$\frac{hf}{U_\infty} \equiv S = \frac{K_A}{2\pi(1 + M_\infty)} ;$$

$$K_A = 1, 2, 3, \ldots \qquad (6)$$

Here, h is the axial distance from leading to trailing edge at a particular mode. A typical frequency spectrum of the noise at $M_\infty = 0.75$ and $Re/ft = 2.0 \times 10^6$ is given in Fig. 6. Measured frequencies converted to Strouhal numbers are presented in Fig. 7.

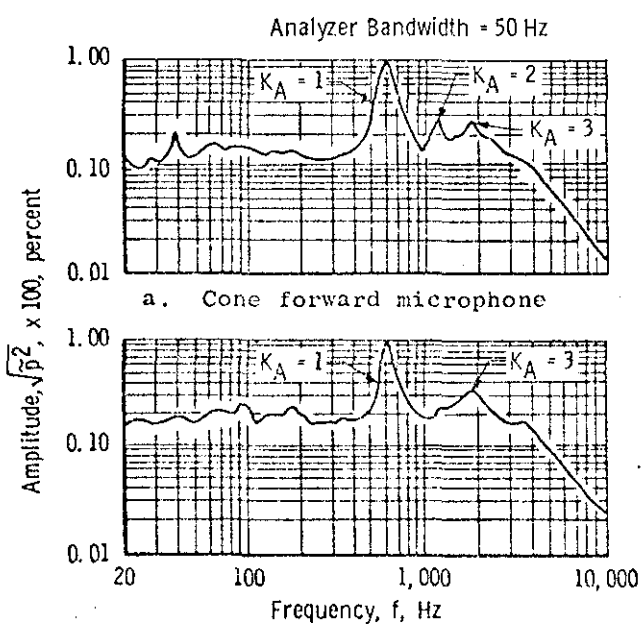

Fig. 6 Noise spectrum in AEDC 16T at $M_\infty = 0.75$, $Re/ft = 2.0 \times 10^6$.

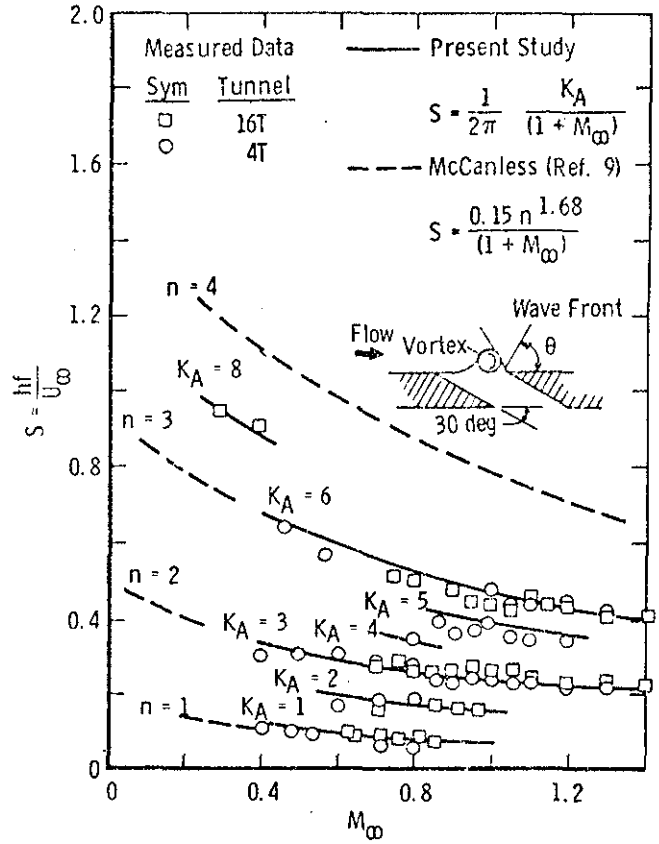

Fig. 7 Edgetone frequencies in the AEDC transonic tunnels.

These results are seen to correspond closely with McCanless' expression in Ref. 9 that

$$S = \frac{0.15\, n^{1.68}}{(1 + M_\infty)}$$

$$n = 1, 2, 3, \text{ or } 4 \qquad (7)$$

McCanless' empirical constant, 0.15 is approximately equal to $1/2\pi$; and the Strouhal numbers coincide for acoustic wave numbers $K_A = 1$, 3, and 6 and the "edgetone stages" n = 1, 2, and 3 defined in Ref. 9. Equation (6), however, explains the intermediate frequencies at $K_A = 2$, 4, 5, and also 8 as belonging to a harmonically related family of tones emanating from the 60-deg inclined holes.

The dependency upon Mach number for edgetone amplitude and frequency is due to wave speed and inclination angle relative to the free-stream flow. This was verified in supporting experiments on perforated wall acoustic characteristics performed in the 6-in. Acoustic Research Tunnel at AEDC. Typical schlieren photos taken in the 6-in. tunnel are shown in Fig. 8 and revealed the test section to be filled with steep-fronted, reinforced, phase-locked plane waves inclined to the flow at the angle

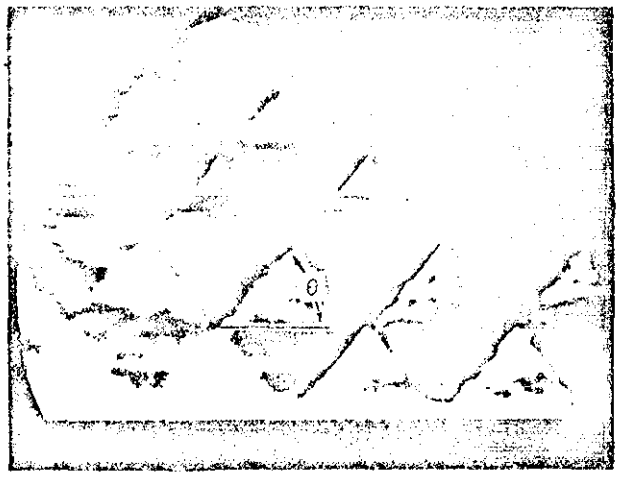

$M_\infty = 0.80$

$M_\infty = 0.90$

Fig. 8 Sound waves from perforated walls at high subsonic Mach numbers.

$$\theta = \sin^{-1} M_\infty \qquad (8)$$

for $0.5 \leq M_\infty \leq 0.9$

$\theta = 45$ deg

for $0.9 < M_\infty \leq 1.0$

$\theta < 45$ deg

for $1.0 < M_\infty \leq 1.1$

(The maximum Mach number capability of the 6-in. tunnel with top and bottom perforated walls and solid side walls for schlieren access was 1.15.) At the resonance conditions in the 6-in. tunnel, the plane waves were seen to coalesce into a well-defined diamond pattern with equal and opposite reflections at the walls. Amplitudes in the 6-in. tunnel generally exceeded those in the full-scale because of the strong reflections at the walls and lack of sufficient distance for appreciable wave attenuation. Amplitudes of the waves shown in Fig. 8 were approximately 156 db. A 1/4-in.-diam 30-deg cone-cylinder model was used for illustration in these photos that steep-fronted sound waves can indeed exist in subsonic flow. (There is no bow shock.) These waves exceed the amplitude limits for acoustic theory and are more properly characterized as "finite" waves.

The edgetones did not register in the hot-film TI data taken in AEDC 16T. They are highly pressure-density coupled with negligible fluctuating velocity at high subsonic and transonic speeds. This observation is in agreement with Spee's results[17] which included schlieren photography, microphone, and hot-wire measurements of similar sound waves. These waves are typical of the nonlinear propagation of "finite-amplitude" disturbances in high-speed flow where the local sound speed varies, causing coalescence of the compressions and a flattening of the rarefactions. A different edgetone pattern of resonance occurs in AEDC 4T as compared to AEDC 16T, although the propagation mechanism is the same, involving edgetone wave numbers $K_A = 3$ and 6 at $M_\infty = 0.819$ ($m = 18$ and 36) and varied modes at varied porosity at the supersonic Mach numbers.

NASA/ARC 11 TWT

The results obtained in the NASA/Ames Research Center 11-ft Transonic Wind Tunnel, ARC 11 TWT, are presented in Fig. 9. Data are presented at unit Reynolds number per foot levels of 2.0×10^6, 3.0×10^6, and 4.0×10^6. The tunnel total temperatures varied between 55 and 90°F as Mach number was increased from 0.4 to 1.2. The unit Reynolds number variation was produced by varying the total pressure. The cone was tested at three different axial positions in the test section, Stations 110, 122, and 150 in. Results are given in Fig. 9 for Stations 110 and 122 in. The results at Station 150 in. were over a smaller Mach number range and are not included. There is a resonance peak at approximately 0.71 Mach number which agrees closely with measurements by Dods and Hanley.[11] Testing at the three axial positions revealed a definite increasing gradient in noise level as the model was moved aft. The noise was found to be dominated by two discrete tones at nominally 2650 and 5300 Hz. A similar procedure of covering the slots with tape to that performed on the AEDC 16T perforated walls revealed these tones to be associated with the slots. The noise gradient with axial position was found to be associated with broadband noise propagated upstream from the diffuser. For the same Mach numbers, lower transition Reynolds numbers are seen in Fig. 9 to accompany higher noise levels at the aft position.

Actual samples of the ARC 11 TWT slotted wall were tested in the 6-in. Acoustic

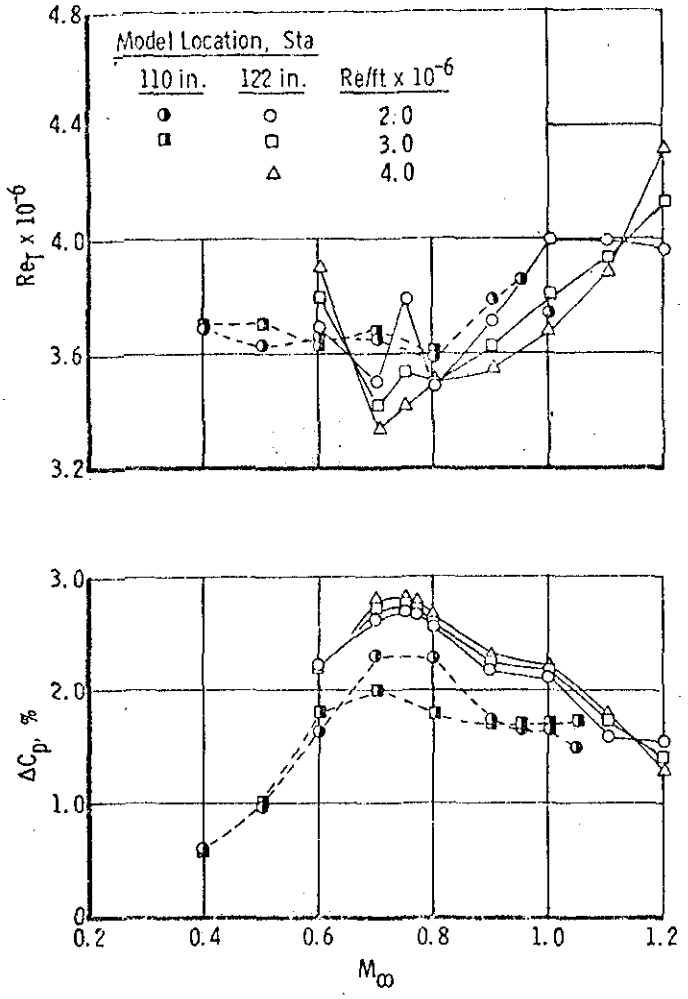

Fig. 9 Noise and Re_T variation in NASA/ARC 11 TWT.

Research Tunnel at AEDC. The samples provided a single slot in top and bottom walls down the center of the 6-in. test section. Frequencies measured by a microphone on the tunnel side wall were the same as those predominant in the full-scale tunnel as shown in Fig. 10, with the addition of a third harmonic. It was found that these frequencies correspond to a half wave organ pipe mode in the corrugated insert in the slot and depend only upon the corrugation depth, d. The organ pipe frequency is given given by the following expression:

$$f = \frac{K_A c_\infty}{2(d + \epsilon)}; \; K_A = 1, 2, 3, \ldots \qquad (9)$$

where ϵ is 0.125 in. with no plenum suction and is zero with plenum section. Assumed here is that the local speed of sound in the slot is approximately that in the free-stream, c_∞, decreasing with increasing Mach number, and that the oscillation in the corrugation is a harmonic standing wave pattern with fluctuating velocity and pressure antinodes 90 deg out of phase. The reflection plane, it is surmised, lies a distance ϵ above the slot with no suction and is drawn down to the slot entrance with suction. Schlieren views in the 6-in.

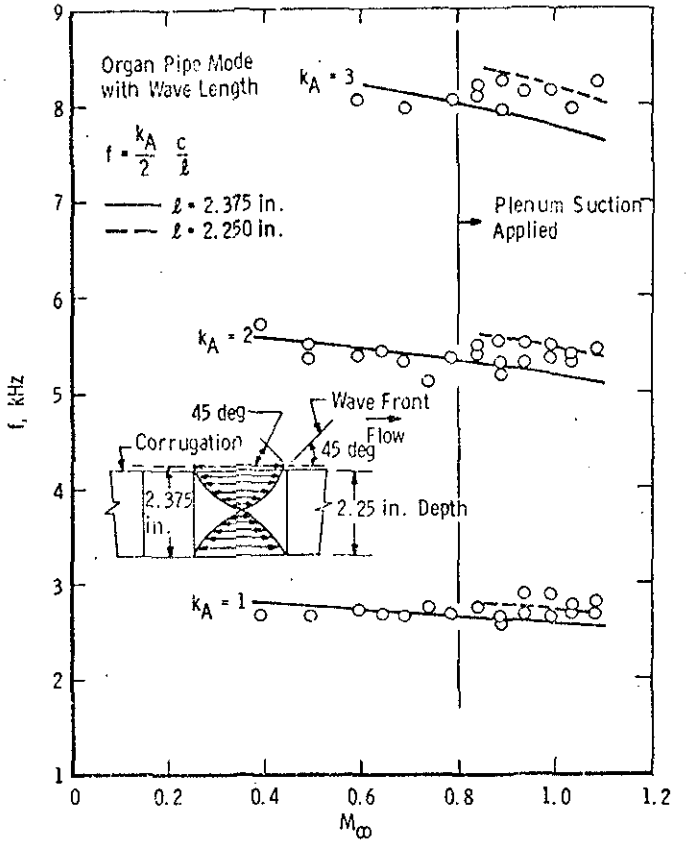

Fig. 10 Organ pipe mode in NASA/ARC 11 TWT slot sample in the 6-in. acoustic research tunnel.

tunnel revealed the wave pattern emanating from the slots also to be composed of steep-fronted phase-locked plane waves, but at a constant 45-deg inclination angle at varied Mach number in contrast to perforated wall edgetones. This is for all subsonic Mach numbers up to 1.0, which was the maximum capability of the 6-in. tunnel with the slotted top and bottom wall samples installed.

NASA/ARC 14 TWT

The 10-deg cone results obtained in the NASA/Ames 14-ft Transonic Wind Tunnel, ARC 14 TWT, are presented in Fig. 11. The ARC TWT being an atmospheric tunnel, these data were acquired at constant total pressure, p_t, of 2130 psfa. However, the total temperature, T_t, varied between 67 and 184°F maximum as Mach number was increased from 0.4 to 1.05. Consequently, the unit Reynolds number per foot increased from approximately 2.6×10^6 at $M_\infty = 0.4$ to approximately 4.0×10^6 maximum near $M_\infty = 0.8$. The experiment with walls taped was again repeated in this tunnel. A trend of increasing noise level and lower transition Reynolds number at each Mach number is evident (particularly above $M_\infty = 0.7$) comparing results with all of the slots taped, only the side walls taped, and the walls fully open. Two discrete tones, associated with the slots, dominated the noise spectra at Mach numbers between 0.7 and 1.05. The frequencies were 1900 and 3300 Hz,

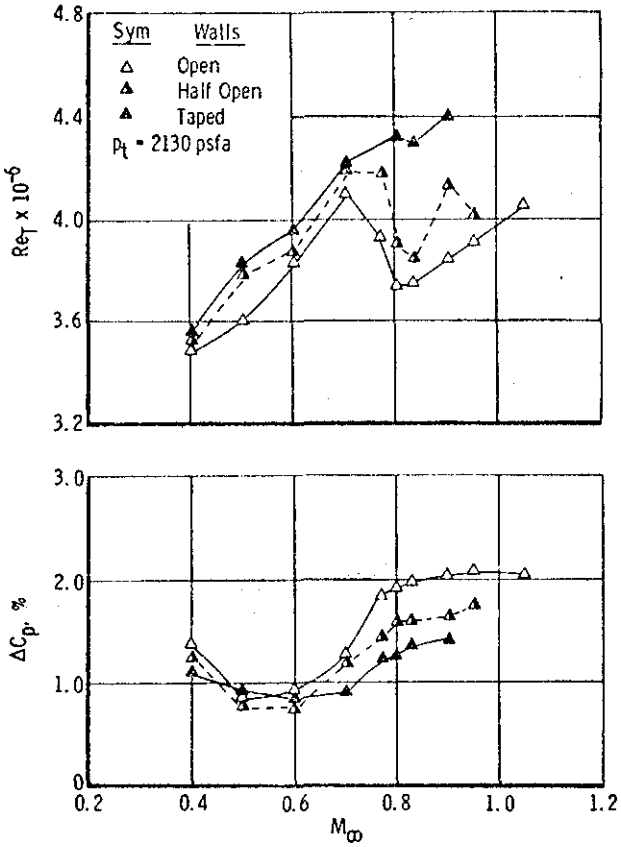

Fig. 11 Noise and Re_T variation in NASA/ARC 14 TWT.

approximately. Although the 3300-Hz tone has not been explained, the 1900-Hz component fits the fundamental organ pipe frequency for a slot corrugation depth of 3.125 in., which is used in the ARC 14 TWT. The slots have essentially the same geometric configuration as in the 11 TWT, only scaled up in the larger tunnel. There is a second major noise source in the ARC 14 TWT, which is of less influence but is dominant at Mach numbers below 0.5. This is the main compressor which has variable drive speed for varied Mach number. Discrete tones in the 135- to 200-Hz range appear in the noise spectra at Mach numbers between 0.4 and 0.5, decreasing in amplitude as Mach number was increased.

NASA/LRC 8 TPT

The 10-deg cone results in the NASA/Langley Research Center 8-ft Transonic Pressure Tunnel, LRC 8 TPT, are presented in Fig. 12. Data were acquired at constant unit Reynolds numbers of 2.0×10^6 and 3.0×10^6. The total temperature was held near constant at 120°F throughout the test, and the total pressure varied to obtain these unit Reynolds numbers. Lower noise levels at Mach numbers greater than 1.0 in the LRC 8 TPT produce significantly higher transition Reynolds numbers than in either the AEDC or the ARC transonic tunnels. And there is a higher transition Reynolds number at 3.0×10^6 unit Reynolds number than at 2.0×10^6 for Mach numbers greater than 0.8, although the ΔC_p levels are approximately the same.

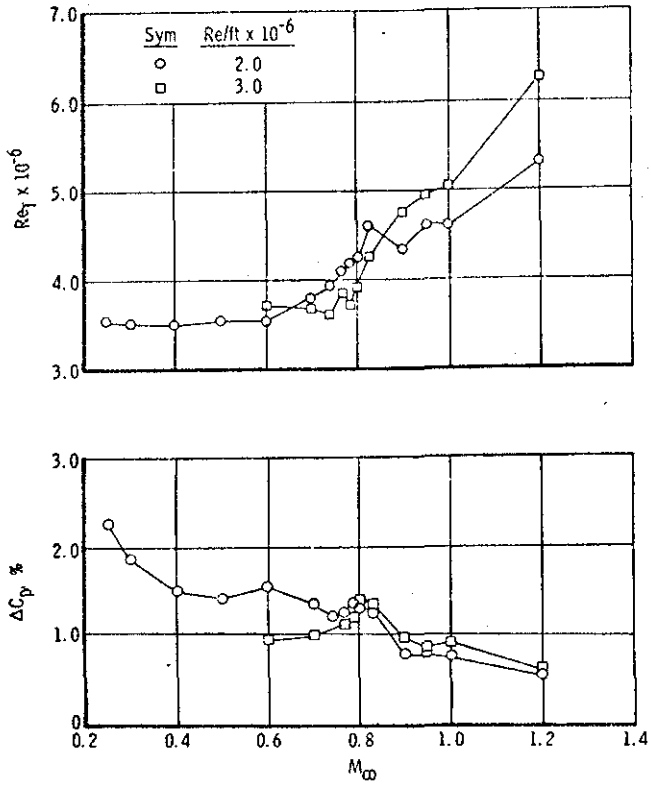

Fig. 12 Noise and Re_T variation in NASA/LRC 8 TPT.

In the Mach number range from 0.25 to approximately 0.5, the 8 TPT has a discrete tone which increases from approximately 3 kHz to approximately 6.5 kHz. This disturbance corresponds to a 26th harmonic of the variable-speed fan, which has 32 rotor blades. There are narrow-band concentrations of disturbances over and above the background at nearly constant frequencies of 4.8 kHz and 10.2 kHz, approximately, at all Mach numbers above 0.7. But the small noise peak to 1.3-percent ΔC_p is associated with growth of the broad-band noise, maximum in the 200- to 300-Hz range, at Mach numbers near 0.8.

NASA/LRC 16TT

The cone results in the NASA/Langley Research Center 16-ft Transonic Tunnel, LRC 16TT (Fig. 13), are generally similar to those in the LRC 8 TPT as shown in Fig. 12. Like the ARC 14 TWT, this is an atmospheric tunnel where p_t was constant at 2120 psfa. The total temperature, T_t, however, varied from 85 to 160°F, giving a unit Reynolds number per foot variation from 1.3×10^6 to 3.9×10^6 as Mach number was varied from 0.3 to 1.3. Transition Reynolds number shows a generally increasing trend with increasing Mach number (or unit Reynolds number), whereas ΔC_p decreases from 1.95 percent at Mach 0.3 to 0.47 percent at Mach

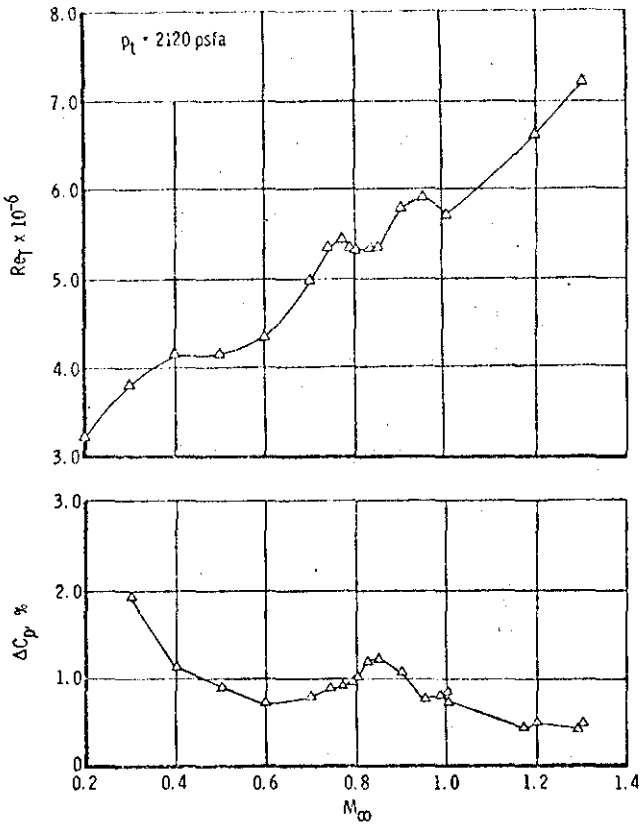

Fig. 13 Noise and Re_T variation in NASA/LRC 16 TT.

1.3. There is a narrow-band concentration of noise at approximately 6 kHz at Mach 0.3, increasing to approximately 7 kHz at Mach 0.4 which may be associated with the counter-rotating, two-stage fan. But, there is nothing distinct in the spectra, except general broad-band increase at frequencies near 10 kHz, to explain the small noise peak to 1.22 percent ΔC_p at Mach 0.85. This tunnel has the lowest disturbance level of all of the tunnels considered through the transonic Mach number range and accordingly, the highest transonic-range transition Reynolds numbers.

V. Correlation of Results

A general trend of the effect of noise on transition is apparent in these data when transition Reynolds numbers are cross-plotted directly against the ΔC_p level. This is only a first-order correlation, ignoring frequency content and directivity. But it is remarkable that a trend should appear even this clearly, considering the broad variation in types of disturbances identified in these six tunnels and the broad variation in test conditions obtained.

The correlation of results in AEDC 4T is given in Fig. 14. Both onset and end of transition Reynolds numbers are shown. The line identified as "predicted onset" is that derived by Benek and High.[18] It is a semiempirical correlation based on the concept put forth by Liepmann and extended by Van Driest and Blumer[19] that

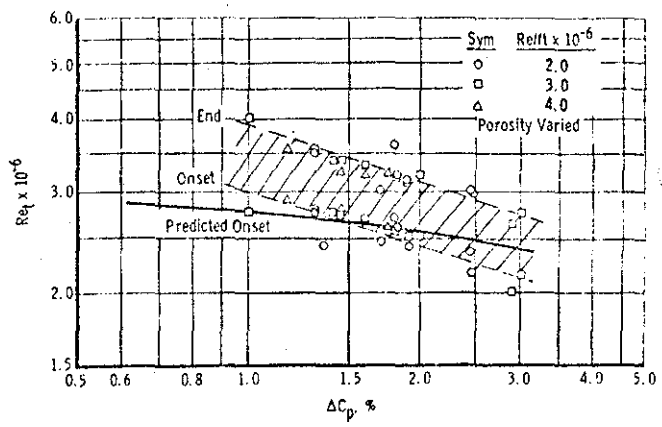

Fig. 14 Data correlation in AEDC 4T.

onset of transition occurs when a critical ratio is achieved between the Reynolds stresses and the viscous stresses present within the laminar boundary layer. For the calculations, the assumptions have been made of adiabatic wall conditions, zero flow angularity, and that the mean axial pressure gradient on the cone is negligible. The analytical expression for transition onset location given in Ref. 18 is as follows:

$$\left(\frac{X_t}{L}\right)^2 - \left[\frac{2K_1}{Re/ft} + \left(\frac{K_1 K_2}{Re/ft}\,\frac{T_w}{T_\infty}\,\Sigma\right)^2\right]$$

$$\left(\frac{X_t}{L}\right) + \left(\frac{K_1}{Re/ft}\right)^2 = 0 \qquad (10$$

where Σ is a disturbance function dominated on the first order by ΔC_p for the 10-deg cone at transonic speeds, T_w is the cone wall temperature, T_∞ is the free-stream static temperature, and L is the 3-ft length of the cone. The constants have empirically assigned values of $K_1 = 1.0$ and $K_2 = 0.0685$ and were weighted heavily by the data acquired in AEDC 16T and the Schubauer-Skramstad result on a flat plate[20] that Re_t approaches 2.85×10^6 in a vanishing turbulence level environment. Results by Spangler and Wells[21] indicate that Re_t approaches 4.9×10^6 at vanishing disturbance level for a smooth flat plate at a low speed. However, flat plate transition results by DeMetz and Casarella[22] in the Naval Ship R & D Center Anechoic Flow Facility at less than 0.1-percent TI are in close agreement with the Schubauer-Skramstad value of 2.85×10^6 for Re_t. The premise is made in Eq. (9) that transition Reynolds number approaches a constant value in the absence of free-stream disturbances. This constant value, with the choice of the constants K_1 and K_2, was therefore taken to be 3.0×10^6, corresponding to a critical value of disturbance Reynolds number, R_{DC}, of 2890.

The correlation of results in AEDC 16T is given in Fig. 15. Onset of transition

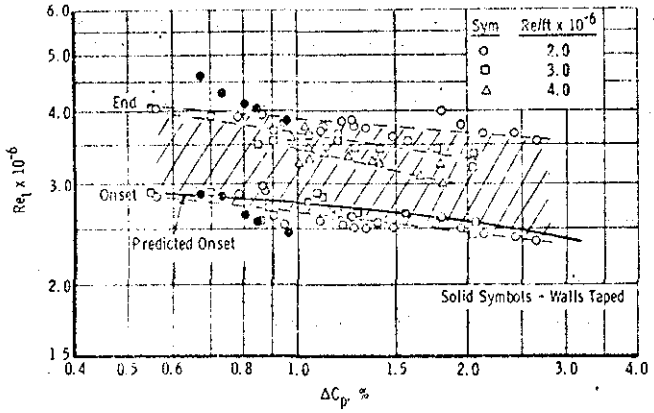

Fig. 15 Data correlation in AEDC 16T.

Reynolds number has a more consistent trend than the end of transition Reynolds number, which is apparently affected by the unit Reynolds number in AEDC 16T. This unit Reynolds number disparity may be due, in part, to an increasing free-stream vorticity level which doubles as unit Reynolds number is increased from 2.0×10^6 to 4.0×10^6 in this tunnel.

The data correlation in the NASA/ARC 11 TWT, Fig. 16, shows reasonably good agreement with the Eq. (10) prediction; however, there is a definite break in the trend curves with a significant increase in both onset and end of transition Reynolds numbers at approximately 0.6 Mach number. The same sort of break occurs in the NASA/ARC 14 TWT data correlation, Fig. 17, again at approximately 0.6 Mach number. No suitable explanation for this break has been found, but the transition data at transonic speeds appear to lie considerably higher than the prediction. In the ARC 14 TWT, when ΔC_p was in the range from 1.5 to 2.0, Re_t values greater than 3.0×10^6 were, in part, the result of experimental error in the minimum pitot profile point caused by the laminar boundary-layer thickness being less than the pitot probe opening height. This would result in a delay in the apparent transition onset point, x_t.

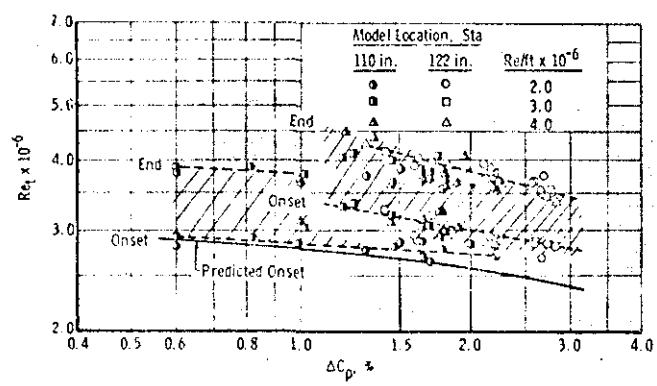

Fig. 16 Data correlation in NASA/ARC 11 TWT.

The NASA/LRC 8 TPT data are correlated in Fig. 18 and exhibit appreciable trend

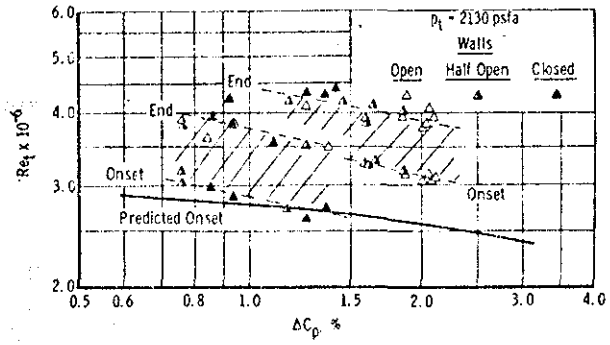

Fig. 17 Data correlation in NASA/ARC 14 TWT.

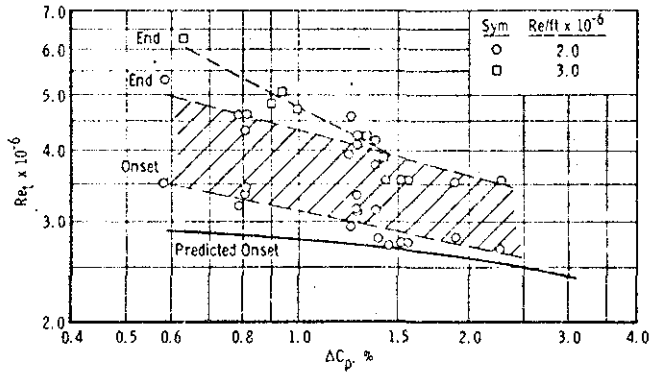

Fig. 18 Data correlation in NASA/LRC 8 TPT.

departure from the prediction at lower noise levels. None of the onset of transition Reynolds number data at 3.0×10^6 unit Reynolds number were considered to be valid, because of experimental difficulties of maintaining good pitot probe contact with the cone surface at the higher unit Reynolds number during this test. Finally, the correlation of results obtained in the LRC 16TT as shown in Fig. 19 exhibits approximately the same rate of change in transition Reynolds number with increasing noise levels as in most of the other tunnels; but the transition Reynolds numbers are much higher than predicted for the levels of ΔC_p measured. A possible explanation is that the noise levels detected by the strain-gage pressure transducers used in the LRC tests were higher than those detected by condenser microphones used in the other tests. Condenser microphones were later adopted as the standard instrumentation for the cone as they were considered to be more reliable in this application.

Aside from the aforementioned observations about possible experimental errors in the data, other factors not accounted for in this analysis are that noise frequency composition was not differentiated, the model vibrations were not considered, the effects of free-stream vorticity level have not been fully evaluated, there could have been appreciable test section flow angularity, and the heat transfer between the cone and the free stream may not have

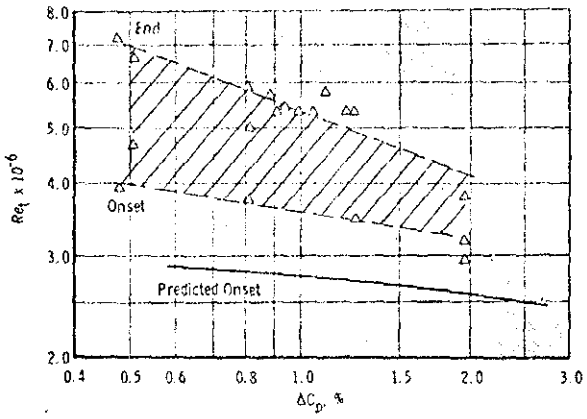

Fig. 19 Data correlation in NASA/LRC 16 TT.

always been negligible. Furthermore, there are basic differences in the mode of operation between the AEDC perforated-wall auxiliary suction, which is applied for Mach numbers of 0.7 or greater, and the NASA slotted-wall flap suction, when the flaps are not opened until the Mach number is 1.0 or greater. (The NASA/LRC 16TT has auxiliary suction on the plenum; but this is likewise not applied until Mach 1.0.) The possibility that appreciable differences in the axial pressure gradient on the cone (buoyance effects) might be introduced by differences in test section construction warrants further evaluation because it introduces a second variable to the experiment which could obscure the desired correlation between noise and transition. The buoyancy effect from positive Mach number gradient would be to delay transition. Full evaluation would entail a critical assessment of the axial Mach number distribution in each tunnel for possible pressure gradient effect on the cone transition results. Buoyancy corrections to aerodynamic test data would be applied separately from a correction for "effective" Reynolds number.

VI. Future Plans

The long-range objective of the study is to obtain the correlation between transition Reynolds number and the aerodynamic disturbances that occur in current-day transonic wind tunnels. This correlation, together with the improved definition of the tunnel flow environment, should afford some measure of improvement to aerodynamic testing in transonic tunnels. The tunnel-to-tunnel correlation is now fairly comprehensive for the continuous-flow tunnels. It is planned that in the future data will also be acquired in several of the blow-down-type U.S. industrial manufacturer transonic tunnels for more extensive transonic test technique comparison.

Inclusion of the supersonic tunnels and data at low Mach numbers down to as low as 0.2 has been to overlap this correlation study with those of others and to place the transonic test regime in perspective with other test regimes. The most recent testing was in April 1974, when the NASA/LRC Transonic Dynamics Tunnel (both in air and in Freon 12® as the test medium) and the Naval Ship R & D Center 7- x 10-ft Transonic Tunnel were added. These two tunnels both use the coarsely spaced slots similar to the NASA/LRC 8 TPT and 16 TT. Additional correlation to the AEDC perforated-wall tunnels was provided by the data acquired in the ONERA 6- x 6-ft transonic tunnel at Modane, France. One other transonic test section configuration has also been included in previous testing: the 22-percent-open normal-hole perforated wall used in the Calspan Corp. 8-ft transonic tunnel and the ARA, LTD., 9- x 8-ft transonic tunnel in the United Kingdom.

Correlation of all of the tunnels to free-flight is planned for the spring of 1975 at Mach numbers from 0.3 to 1.8 at varied altitudes sufficient to obtain transition on the cone. The cone will be flown on a pivoting support boom mounted on the nose of a USAF RF-4C aircraft operated by the 4950th test wing based at Wright-Patterson AFB, Ohio. The flight data will be acquired in straight-and-level flight at zero incidence with the pivoting boom compensation for changes in aircraft attitude.

VII. Concluding Remarks

It has been shown that the transition Reynolds numbers measured on the cone reflect the degradation in dynamic flow quality from aerodynamic noise sources. The comparison of results in these six transonic tunnels reveals significant tunnel-to-tunnel differences at matched test conditions which can affect Reynolds number sensitive parameters in aerodynamic testing. Using transition Reynolds number as the indicator for dynamic flow quality, this means that there are corresponding large differences in the "effective" test Reynolds numbers.

Focus on the areas for greatest facility improvement in dynamic flow quality in these tunnels has been provided. For the perforated-wall tunnels, this would be to eliminate the edgetones without compromising the favorable supersonic wave cancellation properties. For the finely spaced slotted-wall tunnels using corrugated inserts in the slots, this would be to silence the organ pipe mode. As expected, the data show that the combined slotted-perforated features of the slotted walls with corrugated inserts yielded results falling in between the purely perforated- and the purely slotted-wall configurations.

A basis of reference for the wind tunnel-to-free flight correlation should be provided by the cone flight test data. Even if the transition process is never fully understood, use of transition Reynolds number data should provide the means for determining relative "effective" Reynolds numbers in each tunnel upon which to base corrections of test data.

Finally, new insight has been provided for the fundamental correlation of the effect of high-amplitude free-stream disturbances on transition. These aerodynamic noise disturbances in transonic tunnel reaching 2 to 3 percent of the dynamic pressure have a profound effect on transition, even though their frequencies lie well below those predicted to be unstable by linear stability theory. The explanation is possibly due to their great amplitude, far exceeding the fundamental basis for linear stability theory of predicting the growth of infinitesimally small disturbances.

References

[1]Morkovin, M. V., "Critical Evaluation of Transition from Laminar to Turbulent Shear Layers with Emphasis on Hypersonically Travelling Bodies," AFFDL-TR-68-149, March 1969.

[2]Morkovin, M. V., "Open Questions - Transition to Turbulence at High Speeds," Project Themis, AFOSR-70-1731, August 1970.

[3]Mack, L. M., "Boundary-Layer Stability Theory," Jet Propulsion Laboratory, California Institute of Technology No. 900-277, November 1969.

[4]Pope, A., Wind Tunnel Testing, John Wiley and Sons, Inc., 1954.

[5]Czarnecki, K. R. and Sinclair, Archibald R., "Factors Affecting Transition at Supersonic Speeds," RM L53118a, November 1953, NACA.

[6]Pate, S. R. and Schueler, C. J., "Effects of Radiated Aerodynamic Noise on Model Boundary-Layer Transition in Supersonic and Hypersonic Wind Tunnels," AEDC-TR-67-236 (AD666644), March 1968. Also AIAA Paper No. 68-375.

[7]Pate, S. R., "Measurements and Correlations of Transition Reynolds Numbers on Sharp Slender Cones at High Speeds," AEDC-TR-69-172 (AD698326), December 1969.

[8]Karabinus, R. J. and Sanders, B. W., "Measurements of Fluctuating Pressures in 8- by 6-Foot Supersonic Wind Tunnel for Mach Number Range of 0.56 to 2.07," TMX-2009, May 1970, NASA.

[9]McCanless, G. F., "Additional Corrections of 4% Saturn V Protuberance Test Data," TR HSM-R1-71, January 1971, Chrysler Corp.

[10]Credle, O. P., "Perforated Wall Noise in the AEDC-PWT 16-ft and 4-ft Transonic Tunnels," AEDC-TR-71-216 (AD888561L), October 1971.

[11]Dods, J. B. and Hanly, R. D., "Evaluation of Transonic and Supersonic Wind Tunnel Background Noise and Effects on Surface Pressure Fluctuation Measurements," AIAA Paper No. 72-1004, presented at the AIAA 7th Aerodynamic Testing Conference, Palo Alto, California, September 1972.

[12]Cox, R. N. and Freestone, M. M., "Design of Ventilated Walls with Special Emphasis on the Aspect of Noise Generation," Fluid Motion Problems in Wind Tunnel Design. AGARD Report No. 602, No. 6, November 1972.

[13]Mabey, D. G., "Flow Unsteadiness and Model Vibration in Wind Tunnels at Subsonic and Transonic Speeds," CP No. 1155, October 1970, RAE, Bedford, England.

[14]Treon, S. L., Steinle, F. W., Hagerman, J. R., Black, J. A., and Buffington, R. J., "Further Correlation of Data from Investigations of a High-Subsonic-Speed Transport Aircraft Model in Three Major Transonic Wind Tunnels," AIAA Paper No. 71-291, presented at the AIAA 6th Aerodynamic Testing Conference, Alburquerque, New Mexico, March 1971.

[15]Credle, O. P. and Carleton, W. E., "Determination of Transition Reynolds Number in the Transonic Mach Number Range," AEDC-TR-70-218 (AD875995), October 1970.

[16]Uberoi, M. S., "Effect of Wind Tunnel Contraction on Free-Stream Turbulence," Journal of the Aeronautical Sciences, Vol. 23, No. 8, August 1956.

[17]Spee, B. M., "Wind Tunnel Experiments on Unsteady Cavity Flow at High Subsonic Speeds," CP No. 4, 1966, AGARD.

[18]Benek, J. A. and High, M. D., "A Method for the Prediction of the Effects of Free-Stream Disturbances on Boundary-Layer Transition," AEDC-TR-73-158 (AD767899), October 1973.

[19]Van Driest, E. R. and Blumer, C. B., "Boundary Layer Transition: Free-Stream Turbulence and Pressure Gradient Effects," AIAA Journal, Vol. 1, No. 6, June 1963, pp. 1303-1306.

[20]Schubauer, G. B. and Skramstad, H. F., "Laminar-Boundary Layer Oscillations and Transition on a Flat Plate," Report 909 (1948), NACA.

[21]Spangler, J. G. and Wells, C. S., Jr., "Effects of Free-Stream Disturbances on Boundary-Layer Transition." AIAA Journal, Vol. 6, No. 3, March 1968, pp. 543-545.

[22]DeMetz, F. C., and Casarella, M. J., "An Experimental Study of the Intermittent Properties of the Boundary Layer Pressure Field during Transition on a Flat Plate," Naval Ship R & D Center Report No. 4140, November 1973.

12 JUL 1974